JOURNAL OF SOLID STATE CHEMISTRY **112,** 100–105 (1994)

Valence Fluctuation in α-CuVO$_3$ Studied by Photoemission Spectroscopy

M. Nakamura,[1] H. Namatame, and A. Fujimori[2]

Department of Physics, University of Tokyo, Bunkyou-ku, Tokyo 113, Japan

A. Misu

Department of Physics, Science University of Tokyo, Kagurazaka, Shinjuku-ku, Tokyo 162, Japan

and

S. Okatake, M. Onoda, and H. Nagasawa

Institute of Physics, University of Tsukuba, Tennodai, Tsukuba 305, Japan

Received July 16, 1993; in revised form November 17, 1993; accepted November 18, 1993

We have performed a photoemission study of the mixed-valence semiconductor α-CuVO$_3$ (Cu$_{7-x}$V$_6$O$_{19-x}$, $x \sim 0.38$). From the measured spectra we have found that both Cu and V are mixed-valent between Cu$^+$ and Cu^{2+} and between V^{4+} and V^{5+}. The mean valences of Cu and V deduced from the spectra suggest a considerably larger number of local magnetic moments than that deduced from the Curie–Weiss magnetic susceptibility, indicating that the magnetic moments of the V^{4+} and Cu^{2+} ions are partially suppressed. Combining the present results with the NMR and ESR data, we proposed that the V^{4+} local moments are totally suppressed by the formation of singlet pairs and the Cu^{2+} local moments are reduced by the Cu$^+$–Cu^{2+} valence fluctuation. The O 2p to Cu 3d charge-transfer energy deduced from the analysis of the Cu 2p core-level spectrum is found to be small, which may favor the occurrence of the valence fluctuation at the Cu sites. © 1994 Academic Press, Inc.

INTRODUCTION

Cu oxides, which have recently attracted a great deal of attention because of high-T_c superconductivity, are classified into the charge-transfer regime of the Zaanen–Sawatzky–Allen (ZSA) "phase diagram" (1, 2). Valence fluctuation between Cu^{2+} and Cu^{3+} occurs in the hole-doped superconductors, and that between Cu+ and Cu^{2+} in the electron-doped superconductors. V oxides, on the other hand, whose unusual magnetic properties and metal-insulator transitions have been the subject of many studies, are classified into the Mott–Hubbard regime of the ZSA diagram (1, 3). Valence fluctuation between V^{4+} and V^{5+} is reported in, e.g., Na$_x$V$_2$O$_5$ (4). Cu–V ternary oxides, therefore, are expected to show interesting magnetic and electrical properties which result from the complex valence fluctuations involving both the Cu and the V sites. Indeed, unusual structural and transport behaviors have been observed for Cu$_x$V$_2$O$_5$, Cu$_x$V$_4$O$_{11}$, etc. (5).

For α-CuVO$_3$ (Cu$_{7-x}$V$_6$O$_{19-x}$, $x \sim 0.2$–0.3), it was considered that all Cu atoms were divalent and all V atoms were quadruvalent since the charge neutrality is thus fulfilled (6). Chamberland (7), however, concluded that Cu and V were intermediate between Cu$^+$ and Cu^{2+} and between V^{4+} and V^{5+}, respectively, because the effective moment deduced from the static magnetic susceptibility was much smaller than that expected for the pure Cu^{2+} and V^{4+} valence states. The crystal structure of Cu$_{7-x}$V$_6$O$_{19-x}$ (6), which has rhombohedral symmetry, is shown in Fig. 1. The unit formula Cu$_{7-x}$V$_6$O$_{19-x}$ contains six Cu(1) atoms which occupy distorted tetrahedral sites, $1 - x$ Cu(0) atoms which occupy distorted octahedral sites, and six V atoms which occupy distorted octahedral sites. Electrical measurements show semiconducting behavior (6, 7). The number of Cu^{2+} local moments deduced from the Curie constant is incidentally close to the number of Cu(0) sites. This does not mean, however, that the magnetic moments are localized at the Cu(0) sites: In NMR experiments (8), no Cu^{2+} signal has been found, but a single Cu component probably due to intermediate valence Cu atoms has been observed at room temperature, suggesting a Cu$^+$–Cu^{2+} valence fluctuation involving both

---

[1] Permanent address: Department of Physics, Science University of Tokyo.

[2] To whom correspondence should be addressed.

0022-4596/94 $6.00

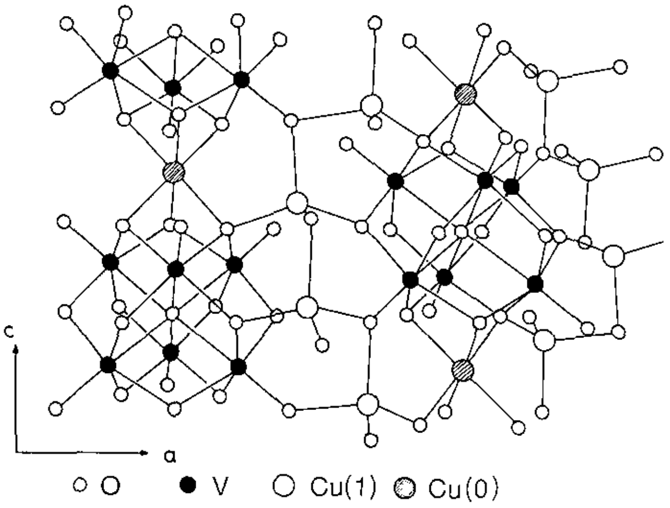

FIG. 1. Crystal structure of Cu$_{7-x}$V$_6$O$_{19-x}$ according to Rea and Kostiner (6).

the Cu(0) and the Cu(1) sites. V NMR results and the g values deduced from ESR experiments imply that all the V ions are nonmagnetic. The Cu and V NMR signals show splitting below $T \sim 220$ K, suggesting a structural phase transition and associated charge redistribution at low temperatures.

Photoemission spectroscopy is a powerful tool for studying the valence states of transition-metal ions in solids. It is a fast probe and provides information which is complementary to that deduced from static magnetic susceptibility, ESR, and NMR measurements. We have performed a photoemission study of Cu$_{7-x}$V$_6$O$_{19-x}$ in order to get more insight into the origin of those anomalous magnetic properties.

EXPERIMENT

We have measured a single crystal of a large size (~10 × 10 × 10 mm^3), which was grown by the Bridgman method. The x in Cu$_{7-x}$V$_6$O$_{19-x}$ was determined to be 0.38 ± 0.11 by electron-probe microanalysis (EPMA; oxygen content could not be determined); namely, the Cu(0) : Cu(1) atomic ratio was 0.62 ± 0.11 : 6, whereas that of Chamberland's sample prepared by the hydrothermal method was $x = 0.22$ (7).

Photoemission and Auger-electron spectra were taken with a spectrometer having a base pressure of ~2 × 10^{-10} Torr equipped with a He discharge lamp for ultraviolet photoemission spectroscopy (UPS) and a Mg X-ray source for X-ray photoemission spectroscopy (XPS). Measurements were made both at room temperature and at liquid-nitrogen temperature. The total instrumental resolution was ~0.2 eV for UPS and ~1 eV for XPS. The satellites of the He and Mg sources have been numerically subtracted. Clean sample surfaces were obtained by scraping *in situ* with a diamond file. The cleanliness of the surface was checked by the absence of a shoulder on the high-binding-energy side of the O 1*s* core-level photoemission peak (see Fig. 5). The C 1*s* core signal, which may arise from surface contamination, was below the detectability limit, i.e., less than several percent of the O 1*s* intensity.

RESULTS

In going from room temperature to liquid-nitrogen temperature, all the XPS and UPS valence-band and core-level spectra except for the V core-level spectra are shifted toward higher binding energy by ~0.2 eV. Although the shifts could be due to a charging effect of the semiconducting sample at low temperature, we believe that they are real shifts associated with the structural phase transition since shifts due to charging will usually occur very differently between UPS and XPS. The constancy of the V core-level binding energies is then real and is not an accidental cancellation of the charging effect and core-level shifts. The shifts of the spectra are presumably associated with the structural phase transition at ~220 K.

Figure 2 shows valence-band UPS (He(II), $h\nu = 40.8$ eV) and XPS (Mg$K\alpha$, $h\nu = 1253.6$ eV) spectra taken at both room temperature and liquid-nitrogen temperature. The density of states at the Fermi level is low without any sign of a Fermi edge, consistent with the semiconducting behavior. The emission at a binding energy of ~2 eV is due to the Cu 3*d* band and that at 3–8 eV is due to the O 2*p* band. The broad emission at ~13 eV is the satellite

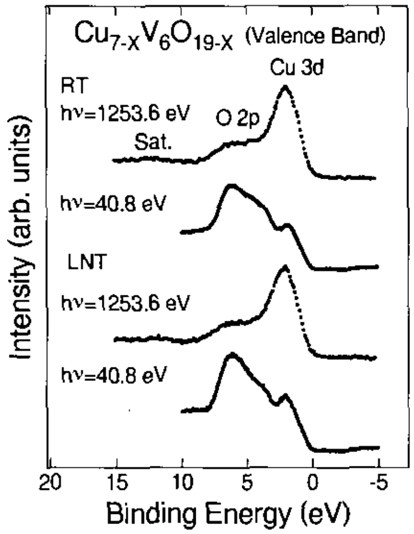

FIG. 2. Photoemission spectra in the valence-band region taken at room temperature (RT) and liquid-nitrogen temperature (LNT).

of Cu^{2+} with the final-state configuration d^8. The relative intensities of these features vary between the XPS and UPS spectra since the Cu 3*d* to O 2*p* relative cross section increases with increasing photon energy (9). Between room temperature and liquid-nitrogen temperature, the spectra do not show significant changes except for the 0.2-eV shift mentioned above. The V 3*d* band is not clearly identified in the XPS or in the UPS spectra, because the photoemission cross section of the V 3*d* orbitals is orders of magnitude smaller than those of the Cu 3*d* and O 2*p* orbitals (9).

The V 3*d* partial density of states in the valence band can be studied by V core–core–valence Auger-electron spectroscopy. Figure 3 shows the V $L_{2,3}M_{2,3}M_{4,5}$ (2*p*–3*p*–3*d*) Auger-electron spectra; they are compared with those of V_2O_5 and VO_2 reported by Sawatzky and Post (10). The peaks at kinetic energies ~473 and ~468 eV are due to the V 3*d* band and the V 3*d* character hybridized into the O 2*p* band, respectively. (O KL_1L_1 Auger-electron emission at kinetic energy ~479 eV overlaps the spectrum. Also, the $L_{2,3}M_{2,3}M_{4,5}$ spectrum consists of the $L_2M_{2,3}M_{4,5}$ and $L_3M_{2,3}M_{4,5}$ components, with the latter being much more intense than the former. The weaker $L_2M_{2,3}M_{4,5}$ component is shifted toward higher kinetic energies by the V 2*p* spin–orbit splitting, ~8 eV, relative to the dominant $L_3M_{2,3}M_{4,5}$ component and overlaps its tail and the O KL_1L_1 feature.) The spectra show that the intensity of the ~473-eV feature due to the V 3*d* band is intermediate between those of $V_2O_5(V^{5+}, 3d^0)$ and $VO_2(V^{4+}, 3d^1)$, indicating that the number of V 3*d* electrons is intermediate between d^0 and d^1, namely, that the valence of V is intermediate between V^{4+} and V^{5+}.

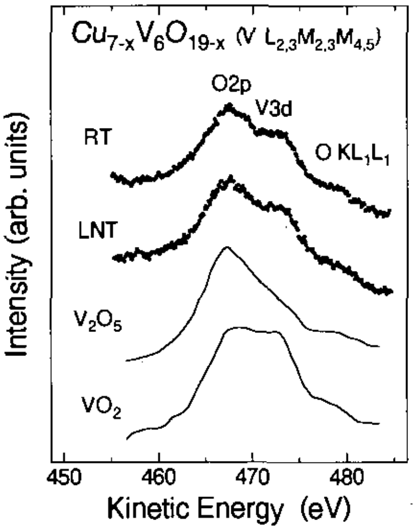

FIG. 3. V $L_{2,3}M_{2,3}M_{4,5}$ Auger-electron spectra. They are compared with those of V_2O_5 and VO_2 reported by Sawatzky and Post (10).

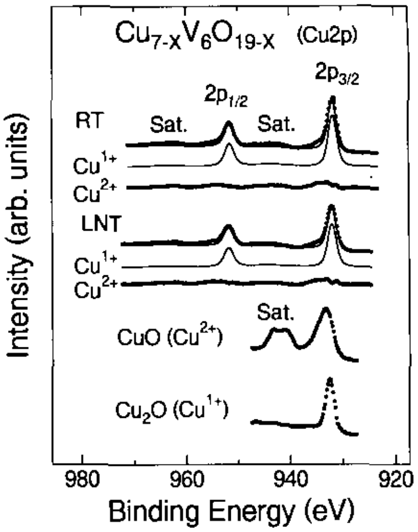

FIG. 4. Photoemission spectra of the Cu 2*p* core level decomposed into the Cu^+ and Cu^{2+} components, compared with the spectra of CuO and Cu_2O reported by Ghijsen *et al.* (11).

Figure 4 shows the Cu 2*p* core-level photoemission spectra compared with those of CuO and Cu_2O reported by Ghijsen *et al.* (11). The most intense peak at binding energy ~932 eV is due to the $\underline{2p_{3/2}}3d^{10}$ final state of Cu^+, and the peak at ~951 eV is its spin–orbit partner $\underline{2p_{1/2}}3d^{10}$. We suppose that the $\underline{2p_{3/2}}3d^{10}\underline{L}$ feature of Cu^{2+} overlaps the $\underline{2p_{3/2}}3d^{10}$ peak of Cu^+ because the observed peak shows a tail on the high-binding-energy side. Here, $\underline{L}$ denotes a ligand hole and $\underline{2p_{3/2}}$ denotes a $2p_{3/2}$ core hole, etc. Indeed, a broad weak feature is observed at ~944 eV where the satellite of Cu^{2+} is expected to appear, indicating the coexistence of Cu^+ and Cu^{2+} in this compound. We have thus decomposed the measured spectra into Cu^+ and Cu^{2+} components by a least-squares fitting: The lineshape of the Cu^+ component has been assumed to be a single spin–orbit doublet whose Gaussian width is set equal to the instrumental resolution and whose Lorentzian width is taken from theoretical calculation (12). We have taken into account an energy-loss satellite accompanying each of the Cu^+ peaks due to the excitation of a valence-electron plasmon. This satellite is reproduced using parameters obtained by fitting the energy-loss satellite of the O 1*s* core-level photoemission spectrum (see Table 1). The Cu^{2+} component shown in Fig. 4 is what has been obtained by subtracting the Cu^+ component from the measured spectrum. In Table 1, we list the binding energies and the relative intensities of various core-level peaks. The intensity ratio $Cu^+ : Cu^{2+}$ obtained from the fitting is $2.9 \pm 0.2 : 1$, meaning that the mean valence of Cu is 1.25 ± 0.03. Combining this number with the atomic ratio Cu(0) : Cu(1) = $1 - x : 6 = 0.62 \pm 0.11 : 6$, only the following combinations of the Cu valences are possible: (i) Cu(0) is divalent and Cu(1) is mixed-valent, (ii) Cu(0)

TABLE 1
Binding Energies and the Intensities of Core-Level Peaks and the Energy and Width of the Electron Energy-Loss Peak

	Room temperature	Liquid-nitrogen temperature
Binding energy		
Cu^+ $2p_{3/2}$	931.7	931.9
Cu^{2+} $2p_{3/2}$	933.7	933.9
V^{4+} $2p_{3/2}$	516.0	516.0
V^{5+} $2p_{3/2}$	517.6	517.6
Intensity ratio		
$Cu^+ : Cu^{2+}$	1:2.9	1:2.9
$V^{5+} : V^{4+}$	1:1.2	1:1.2
Cu^{2+} Main-satellite separation	11.9	11.9
Energy-loss peak energy	12.3	12.3
Gaussian FWHM	5.0	5.0
Lorentzian FWHM	7.8	7.8

Note. All energies are in eV.

is monovalent and Cu(1) is mixed-valent, or (iii) both Cu(0) and Cu(1) are mixed-valent. That is, Cu(1) cannot be pure Cu^+ nor pure Cu^{2+} but has to be mixed-valent.

Figure 5 shows the V $2p$ and O $1s$ core-level photoemission spectra. The V $2p_{3/2}$ and $2p_{1/2}$ peaks at binding energies 516 and 524 eV consist of overlapping V^{4+} and V^{5+} components. We have again decomposed the spectra into the two components using the least-squares fitting procedure as shown in Fig. 5. Thus the ratio $V^{4+} : V^{5+}$ is found to be $\sim 1.2:1$, yielding the mean valence of 4.45 ± 0.15 for V. This value is considerably smaller than 4.83 ± 0.05 calculated from the mean valences of Cu and the chemical composition $Cu_{7-x}V_6O_{19-x}$ ($x = 0.38 \pm 0.11$) assuming O^{2-}. A likely cause for the discrepancy is the final-state effect in V core-level photoemission: The intensity of the $2p3d^0$ final state (corresponding to the V^{5+} component) is transferred to the $2p3d^1$ final state (V^{4+} component) through the transfer of electrons from neighboring V sites induced by the core-hole potential. Similar phenomena have been found for the V $2p$ core-level spectra of $Li_xZn_{1-x}V_2O_4$ (13). The Lorentzian width of the V^{5+} peaks is larger than that of V^{4+}, indicating that the $2p3d^0$ final state has a shorter lifetime owing to the above screening channel. It should be noted that if there were no d electrons in the V $3d$ orbitals, i.e., if all the V ions are in the V^{5+} state, only the single V^{5+} component must be observed (10). The present V $2p$ XPS spectra thus unambiguously show the existence of V^{4+} states in $Cu_{7-x}V_6O_{19-x}$.

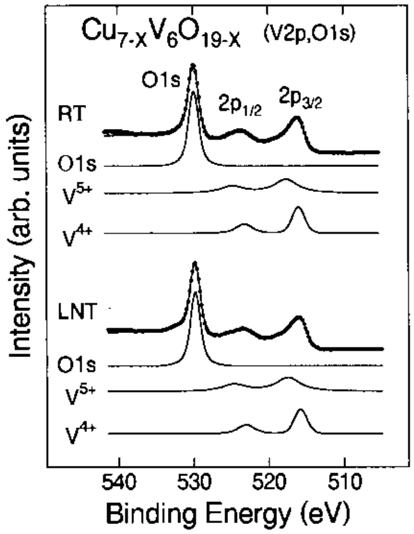

FIG. 5. Photoemission spectra of the V $2p$ core level decomposed into the V^{5+} and V^{4+} components.

DISCUSSION

Interpretation of the Core-Level Photoemission Spectra

We have pointed out that the mean valence of V may not be deduced quantitatively from the V core-level spectra due to the charge transfer between V sites, whereas such a core-hole screening channel is assumed to be negligible for Cu. In principle, charge transfer between Cu sites could occur and therefore the mean valences of Cu obtained from the above fitting only gives a lower limit since the transfer of spectral intensity occurs from Cu^{2+} to Cu^+ peaks. However, this effect should be negligibly small since the $3d$ orbitals of Cu are almost filled and the overlap between the neighboring Cu $3d$ orbitals via intervening O $2p$ orbitals is much smaller. Even if the charge transfer between Cu sites were not negligible, the present conclusion that Cu(1) is not monovalent but is mixed-valent would not be altered since the mean valence of Cu would further increase if such a correction were made.

A satellite associated with a ligand to $3d$ charge transfer is not clearly observed for the V $2p$ core level contrary to the Cu $2p$ core level. In principle, such a satellite exists but its intensity would be very low because of the large ligand–V $3d$ transfer integrals, the large number of unoccupied d states into which the charge transfer occurs, and the relatively weak core-hole–$3d$-electron Coulomb interaction compared to that for heavier $3d$ elements. The overlap of the O $1s$ core-level peak on the higher binding energy side of the V $2p$ peaks further obscures satellite features even if they existed. De Boer *et al.* (14) proposed an exciton mechanism to explain the satellite structures observed in the core-level photoemission spectra of early $3d$ transition-metal compounds. Examination of the validity of the various models for the core-level satellite structures is to be made in future.

Valences of Cu and V and the Magnetic Properties

The existence of V^{4+} concluded from the photoemission study is apparently inconsistent with the nonmagnetic behavior of the V ions suggested by V NMR (8). Presumably two adjacent V^{4+} ions form singlet pairs since such singlet pairing has been observed in $Na_xV_2O_5$ and VO_2 in which edge-sharing VO_6 octahedra constitute the crystal structure as in $Cu_{7-x}V_6O_{19-x}$.

The effective moment due to Cu^{2+} and V^{4+} deduced from the mean valence of Cu obtained by photoemission is 1.18 ± 0.06 μ_B/V (using g = 2.2 deduced from ESR (8)), which is significantly larger than the value 0.60 μ_B/V deduced from the static magnetic susceptibility (8). This means that a considerable number of V^{4+} and Cu^{2+} ions become nonmagnetic, e.g., through the formation of spin–singlet pairs or valence fluctuation. If all the V^{4+} ions became nonmagnetic but Cu^{2+} retained the local moment, the effective moment would be reduced to 0.92 μ_B/V.

We have shown above that despite the uncertainties in the composition x and in the valence of Cu(0), the Cu(1) atoms should be in a Cu^+–Cu^{2+} mixed-valence state. The fact that only one component has been detected in the Cu NMR experiment above $T \sim 220$ K (8) indicates that the Cu^+–Cu^{2+} mixed valence is due to a dynamical valence fuctuation involving both the Cu(0) and the Cu(1) sites and is responsible for the electrical transport at room temperature. The valence fluctuation may further reduce the effective moment arising from the Cu^{2+} ions.

We did not observe any significant change in the photoemission spectra between room temperature and liquid-nitrogen temperature except for the small energy shifts, indicating that the mixed-valence ratio does not change at least between room temperature and liquid-nitrogen temperature, although the singlet pairing and/or the dynamics of the valence fluctuation may change with temperature.

Cu 3d–O 2p Covalency

One can study the local electronic structure of the Cu^{2+} ion and its O^{2-} ligands from analysis of the Cu^{2+} component of the Cu 2p spectra using the cluster model proposed by van der Laan *et al.* (16). That is, by using the model, three parameters T, Q, and Δ can be obtained from the energy separation and the intensity ratio between the main and satellite peaks. Here, T is the transfer integral between the $3d^9$ and $3d^{10}\underline{L}$ states, Q is the Coulomb repulsion energy between the core holes and the 3d hole, and Δ is the charge-transfer energy, i.e., the energy difference between the $3d^9$ and $3d^{10}\underline{L}$ states. In order to obtain values for T, Q, and Δ, we followed the procedure of van der Laan *et al.* (16); that is, we assumed Q to be nearly identical between different Cu^{2+} compounds, including Cu dihalides studied in (16). Parameter values thus obtained are listed in Table 2. Here it should be noted that the observed Cu^{2+} spectrum is a weighted average of those for the Cu^{2+} ions at the Cu(1) and Cu(0) sites and therefore that the deduced parameter values are certain averages of Cu(1) and Cu(0). From Table 2, one can see that the Δ of $Cu_{7-x}V_6O_{19-x}$ is small as in CuO (11) (even smaller than T), indicating strong covalency between the Cu 3d and the O 2p orbitals. In $Cu_{7-x}V_6O_{19-x}$, therefore, the Cu^{2+} state has a d electron number well exceeding nine, which reduces the difference in the net d-electron number between the Cu^+ and Cu^{2+} states and would thus facilitate the occurrence of the Cu^+–Cu^{2+} valence fluctuation.

TABLE 2

Charge-Transfer Energy Δ, Transfer Integral T, and Core-Hole–3d-Hole Coulomb Repulsion Energy Q for $Cu_{7-x}V_6O_{19-x}$ and CuO.

	Δ	Q	T
$Cu_{7-x}V_6O_{19-x}$	1.6 ± 0.2	9.1 ± 0.2	2.5 ± 0.3
CuO[a]	1.55	9.0	2.5

Note. All energies are in eV.

[a] Ref. (10).

CONCLUSION

We have found that both Cu and V are mixed-valent between Cu^+ and Cu^{2+} and between V^{4+} and V^{5+}, respectively. The Cu and V valences obtained from the photoemission spectra yield a number of local magnetic moments that is much larger than the deduced from the static magnetic susceptibility, meaning that the local-moment behavior of Cu^{2+} and V^{4+} ions is partially suppressed. The valence of Cu is dynamically fluctuating between Cu^+ and Cu^{2+} at least at room temperature, and the local-moment behavior of the Cu^{2+} ions is thus partially suppressed. The local-moment behavior of the V^{4+} ions is totally suppressed probably due to the formation of spin–singlet pairs. From the analysis of the satellite structure of the Cu^{2+} XPS spectra, Δ is found to be small as in CuO. Thus the covalency between the Cu 3d and O 2p states is strong in $Cu_{7-x}V_6O_{19-x}$, which leads to similar charge distribution for the Cu^+ and Cu^{2+} states and may facilitate the Cu^{2+}–Cu^+ valence fluctuation. The valence-band and core-level spectra except for the V core levels are shifted by 0.2 eV toward higher binding energy in going from room temperature to ~80 K, possibly associated with the structural phase transition detected by the NMR experiment.

ACKNOWLEDGMENT

This work was supported by a Grant-in-Aid for Scientific Research from the Ministry of Education, Science, and Culture, Japan.

REFERENCES

1. J. Zaanen and G. A. Sawatsky, *Can. J. Phys.* **65,** 1262 (1987); J. Zaanen, G. A. Sawatsky, and J. W. Allen, *Phys. Rev. Lett.* **55,** 418 (1985).
2. A. Fujimori, E. Takayama-Muromachi, Y. Uchida, and B. Okai, *Phys. Rev. B* **35,** 3814 (1987).
3. S. Shin, S. Suga, M. Taniguchi, M. Fujisawa, H. Kakizaki, A. Fujimori, H. Daimon, Y. Ueda, K. Kosuge, and S. Kachi, *Phys. Rev. B* **41,** 4993 (1990).
4. H. Nagasawa, M. Onoda, Y. Kanai, and S. Kagoshima, *Synth. Met.* **19,** 971 (1987) and references therein.
5. Y. Saito, M. Onoda, and H. Nagasawa, *J. Phys. Soc. Jpn.* **61,** 3865 (1992).
6. J. R. Rea and E. Kostiner, *J. Solid State Chem.* **7,** 17 (1973).
7. B. L. Chamberland, *J. Solid State Chem.* **1,** 138 (1970).
8. M. Onoda, Y. Saito, T. Naka, and H. Nagasawa, in preparation.
9. J. J. Yeh and I. Lindau, *At. Data Nucl. Data Tables* **32,** 1 (1985).
10. G. A. Sawatzky and D. Post, *Phys. Rev. B* **20,** 1546 (1979).
11. J. Ghijsen, L. H. Tjeng, J. van Elp, H. Eskes, J. Westerink, and G. A. Sawatzky, *Phys. Rev. B* **38,** 11322 (1988).
12. M. O. Krause and J. H. Oliver, *J. Phys. Chem. Ref. Data* **8,** 329 (1988).
13. A. Fujimori, K. Kawakami, and N. Tsuda, *Phys. Rev. B* **38,** 7889 (1988).
14. D. K. G. de Boer, C. Hass, and G. A. Sawatsky, *Phys. Rev. B* **29,** 4401 (1984).
15. R. D. Shannon and C. T. Prewitt, *Acta. Crystallogr. Sect. B* **25,** 925 (1969).
16. G. van der Laan, C. Westra, C. Hass, and G. A. Sawatzky, *Phys. Rev. B* **23,** 4369 (1981).